

Numerical Simulation of Tsunamis Induced by Rigid Landslide Using MPS-DEM Coupled Method

Fengze Xie¹, Jian Wang², Decheng Wan^{1*}

¹Computational Marine Hydrodynamics Lab (CMHL), School of Naval Architecture, Ocean and Civil Engineering, Shanghai Jiao Tong University, Shanghai, China

²Marine Design & Research Institute of China, Shanghai, China

*Corresponding author

ABSTRACT

The tsunamis induced by rigid landslides such as ice and rock may affect the safety of nearshore floating structures, since the generated waves tend to be strongly non-linear. In this work, a fully Lagrangian meshless method MPS-DEM is developed to solve the fluid–solid interaction problem. The improved moving particle semi-implicit (MPS) method is applied to simulate the incompressible fluid flow, while the Discrete Element Method (DEM) is used to build the solid-ramp interaction. The MPS-DEM coupled method is applied to simulate the subaerial rigid landslide-tsunamis. Numerical results agree well with experimental results.

KEY WORDS: Moving particle semi-Implicit method; Discrete element method; MPS-DEM coupled method; Rigid landslides.

INTRODUCTION

Landslides often occurs on the ramps near the ocean, rivers and reservoirs. Blocking of the rivers by the falling stones leads to dramatic change of environment. Besides, non-linear waves induced by landslides may pose a threaten to the safety of nearshore structures and people. Therefore, it is necessary to investigate the movement of landslides and the propagation of waves.

Model experiment is one of mainly approach to evaluate the influence caused by landslides. Heinrich (1992) conducted experiments to study the surge induced by submarine and aerial landslides. The wave profile and the trajectory of solid bodies was investigated. Lin et al. (2015) experimentally investigated the interaction between the landslide-induced surge wave and a dam. Heller et al. (2016) carried out a 3-D experiment to investigate the surge induced by subaerial landslides. These model experiments mentioned above are usually used to verify the accuracy of numerical methods.

With the development of the computer hardware, many numerical techniques have been proposed for the simulation of complex flows. Particle-based methods show their superiority to capture the free-

surface with large deformation. Weakly Compressible Smoothed Particle Hydrodynamics (WCSPH) method was firstly proposed by Gingold and Monaghan (1977) for the problem of astrophysics. Then, SPH was widely applied for the problem of violent flows. In a few decades, Koshizuka and Oka (1996) developed Moving Particle Semi-implicit (MPS) method to simulated the incompressible flows. There were some draw backs for particle-based methods, such as pressure oscillation and low computational efficiency. High order schemes (Khayyer et al.,2011; Liu et al., 2019; Duan et al., 2021) for gradient model and Laplacian model were developed to enhance the performance of particle-based method. Particle Shifting Technique (PST) (Xu et al, 2009; Khayyer et al, 2017; Duan et al., 2018; Sun et al, 2019a) was also proposed to avoid errors and numerical oscillation brought by uneven distribution of particles. With the help of multi-resolution techniques (Sun et al., 2019b), parallel technique and GPU acceleration technique (Xie et al., 2020), the computational efficiency was improved obviously. With the efforts of several researchers, particle-based methods have been applied to solve more complicated problems, such as multi-phase flows (Khayyer et al., 2019, Wen et al., 2021, Xie et al., 2021b), fluid-structure interaction (Khayyer et al., 2021; Gotoh et al, 2021; Zhang et al., 2021b; Xie et al., 2021a) and flows passing through porous structures (Wen et al., 2018; Khayyer et al., 2018).

The particle-based method was also used to simulate the landslide process. In the traditional strategy, the velocity and the trajectory of landslide was prescribed according to the experimental results before the simulation (Tan and Chen, 2017). However, the effect of the fluid to the slides was ignored and it is difficult to investigate other landslide processes without experimental results. Many approaches were introduced to SPH for the slide-ramp interaction. Yeylaghi et al. (2016) arranged a layer of fluid particles on the interface between the slide and the ramp in. The velocity and displacement of interface fluid particles were updated according to movement of the slide. The hydrodynamics exerted on the slide were calculated by integral of pressure on the slide boundary particles. However, the friction of slide-ramp was not considered and the velocity measured by SPH was slightly higher than that by experiment. Zhang et al. (2021a) introduced a Rigid Slide

Motion Model (RSMM) to the WCSPH framework. The velocity and displacement of the slide measured by WCSPH-RSMM was in good agreement with experimental results. Qi et al. (2022) carried out the simulation of multi-bodies slides by adopting an improved dynamic boundary condition.

Discrete Element Method (DEM) was usually used to build the solid-solid interaction and successfully applied to the simulation of large-scale landslide (Zhou et al., 2021). The DEM was also coupled with SPH, in which DEM was used to model the interaction between rigid slide and ramp. Tan et al. (2018) coupled proposed a 2-D SPH-DEM model and take the advantages of DEM to model the slide-ramp interaction. The hydrodynamics applied on the block are empirical and the numerical results may be affected due to the selection of some parameters. Xu and Dong (2021) developed a 3D SPH-DEM method to simulate multi-bodies slides. Dynamic Boundary Particles (DBPs) was adopted to couple the DEM brocks and SPH particles.

In this work, a new MPS-DEM coupled scheme for the simulation of landslides is developed. Firstly, the improved MPS method, the DEM method and MPS-DEM coupled strategy are introduced briefly. Secondly, two test cases, including the subaerial landslide and submarine landslide, are simulated and compared with experimental results to verify the MPS-DEM model.

NUMERICAL METHOD

MPS formulation for fluid dynamics

The governing equations of the fluid involves mass conservation equation and momentum conservation equation, given by,

$$\nabla \cdot \mathbf{u} = 0 \quad (1)$$

$$\frac{D\mathbf{u}}{Dt} = -\frac{1}{\rho} \nabla P + \nu \nabla^2 \mathbf{u} + \mathbf{g} \quad (2)$$

where the \mathbf{u} , t , ρ , P , ν and \mathbf{g} represent the velocity vector, time, fluid density, pressure, kinematic viscosity of the fluid and gravity acceleration vector, respectively.

The kernel function reflects the interaction strength of particles. A kernel function (Zhang et al., 2014), which can avoid the singular point, is employed here.

$$W(r) = \begin{cases} \frac{r_e}{0.85r + 0.15r_e} - 1 & 0 \leq r < r_e \\ 0 & r_e \leq r \end{cases} \quad (3)$$

Terms in the governing equations as discretized as follows,

$$\langle \nabla \phi \rangle_i = \frac{d}{n^0} \sum_{j \neq i} \frac{\phi_j + \phi_i}{|\mathbf{r}_j - \mathbf{r}_i|^2} (\mathbf{r}_j - \mathbf{r}_i) \cdot W(|\mathbf{r}_j - \mathbf{r}_i|) \quad (4)$$

$$\langle \nabla \cdot \mathbf{u} \rangle_i = \frac{d}{n^0} \sum_{j \neq i} \frac{(\mathbf{u}_j - \mathbf{u}_i) \cdot (\mathbf{r}_j - \mathbf{r}_i)}{|\mathbf{r}_j - \mathbf{r}_i|^2} W(|\mathbf{r}_j - \mathbf{r}_i|) \quad (5)$$

$$\langle \nabla^2 \phi \rangle_i = \frac{2d}{n^0 \lambda} \sum_{j \neq i} (\phi_j - \phi_i) W(|\mathbf{r}_j - \mathbf{r}_i|) \quad (6)$$

where ϕ represents the physical quantity carried by MPS particles, d is the number of space dimension, n^0 is the initial particle density, \mathbf{r} is

the position vector relative to origin, λ is a parameter to make the increase of variance equal to the corresponding analytical solution (Koshizuka and Oka, 1996), given by,

$$\lambda = \frac{\sum_{j \neq i} W(|\mathbf{r}_j - \mathbf{r}_i|) \cdot |\mathbf{r}_j - \mathbf{r}_i|^2}{\sum_{j \neq i} W(|\mathbf{r}_j - \mathbf{r}_i|)} \quad (7)$$

Pressure information is obtained by solving the Pressure Poisson Equation (PPE). In order to balance between stability and accuracy, a mixed source method (Tanaka et al., 2010; Khayyer and Gotoh, 2011) is adopted, defined by,

$$\langle \nabla^2 p^{k+1} \rangle_i = (1 - \gamma) \frac{\rho}{\Delta t} \nabla \mathbf{u}_i^* - \gamma \frac{\rho}{\Delta t^2} \langle n^* \rangle_i - n^0 \quad (8)$$

DEM formulation for solid contact

In the traditional DEM theory, the motion of particle is governed by Newton's second law. However, the velocity and displacement DEM particle will not be updated after calculating the contact force in this work. The contact force is calculated based on the contact model, which consists of springs, dashpots and sliders. The DEM particles are regarded as soft spheres and they can overlap with each other. The overlap is equal to the deformation of the springs. The contact force \mathbf{F}_c can be decomposed into the normal component \mathbf{F}_c^n and tangential component \mathbf{F}_c^t . Both components consist of elastic force and damping force.

$$\mathbf{F}_c^n = -k\delta^n - d\Delta \mathbf{v}^n \quad (9)$$

$$\mathbf{F}_c^t = \begin{cases} -k\delta^t - d\Delta \mathbf{v}^t & (|\mathbf{F}_c^t| < \mu |\mathbf{F}_c^n|) \\ -\mu |\mathbf{F}_c^n| \cdot \Delta \mathbf{v}^t / |\Delta \mathbf{v}^t| & (|\mathbf{F}_c^t| \geq \mu |\mathbf{F}_c^n|) \end{cases} \quad (10)$$

where k and d are the spring constant and damping coefficient, δ^n and δ^t are the normal and tangential relative displacement, $\Delta \mathbf{v}^n$ and $\Delta \mathbf{v}^t$ are normal and tangential relative velocity, μ the friction coefficient.

MPS-DEM coupled model

The MPS-DEM coupled strategy is shown in Fig. 1. The rigid landslide is regarded as the floating body as previous work (Zhang and Wan, 2017). The motion of rigid landslide is governed by,

$$\begin{cases} M \frac{d\mathbf{V}_G}{dt} = M\mathbf{g} + \mathbf{F}_c^L + \mathbf{F}_h \\ I_G \frac{d\boldsymbol{\omega}_G}{dt} = \mathbf{T}_c^L + \mathbf{T}_h \end{cases} \quad (11)$$

where M and I_G are the mass and inertial moment of the rigid landslide, \mathbf{V}_G and $\boldsymbol{\omega}_G$ are the linear and angular velocity in the gravity center of the rigid landslide, \mathbf{F}_c^L and \mathbf{T}_c^L are the total contact force and moment applied to rigid landslide.

The wall particles have both characteristics of MPS and DEM. The

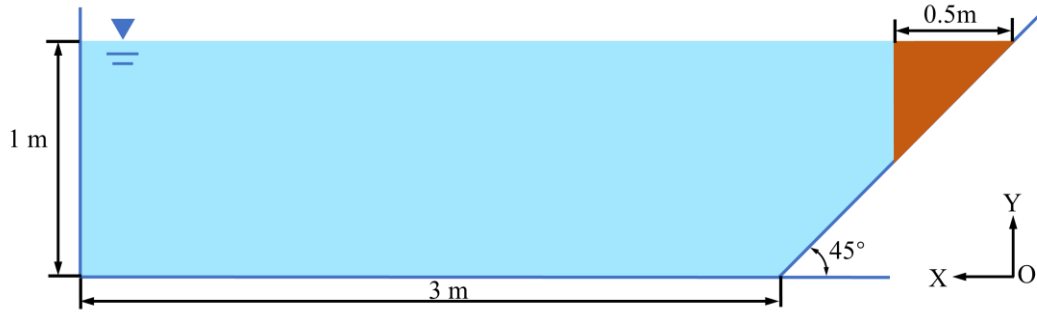


Fig. 2 Sketch of the numerical model for submarine rigid landslide

solid-solid contact force and moment is transferred from DEM particles to the MPS floating bodies, given by,

$$\mathbf{F}_c^L = \sum_k^{Nd} \mathbf{F}_{c,k} \quad (12)$$

$$\mathbf{T}_c^L = \sum_k^{Nd} \mathbf{r}_{G,k} \times \mathbf{F}_{c,k} \quad (13)$$

where the subscript k represents the DEM particle, N_d is the number of DEM particles attached to the floating body, \mathbf{r}_G is the position vector relative to the gravity center. \mathbf{F}_c is the total contact force exerted on each DEM particle.

The hydrodynamics and hydraulic moment exerted on the floating bodies is calculated by the integral of fluid pressure.

$$\mathbf{F}_h = -\sum_i^{N_w} p_i \cdot \mathbf{n}_i \Delta s_i \quad (14)$$

$$\mathbf{T}_h = -\sum_i^{N_w} \mathbf{r}_{G,i} \times (p_i \cdot \mathbf{n}_i \Delta s_i) \quad (15)$$

where \mathbf{F}_h is the total hydrodynamics applied to the floating body, N_w is the number of wall particle, p_i is the pressure of wall particle i , \mathbf{n}_i is the unit normal vector, Δs_i is the area of virtual panel.

The DEM particles do not update their velocity and displacement after obtaining the contact forces, and move with the motion of rigid landslide.

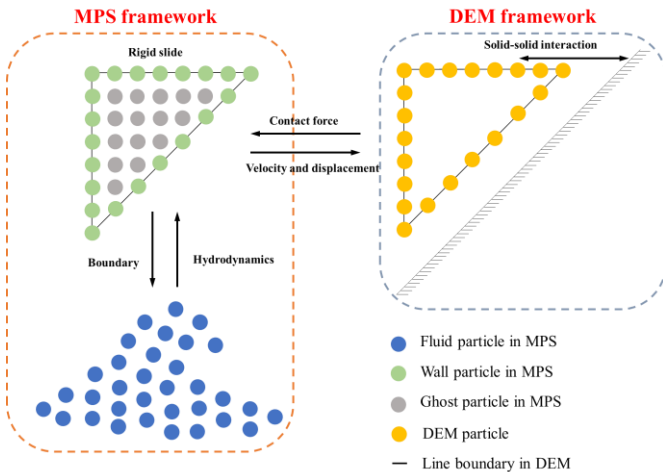


Fig. 1 MPS-DEM coupled strategy

NUMERICAL RESULTS

Submarine rigid landslide

In this sub-section, the experiment of submarine landslide carried out by Heinrich (1992) employed to verify the accuracy of MPS-DEM model. Fig. 2 presents the sketch of the numerical model. The water depth is 1m. A rigid landslide with the cross-section being a wedge is placed at a ramp with a slope angle of 45 degrees. The density of the wedge is 2000 kg/m³. Other parameters of the simulation are presented in the Tables 1 and 2 in detail.

Table 1. MPS parameters in the simulation of submarine rigid landslide

Parameter	Unit	Value
Fluid density	kg/m ³	1000
Kinematic viscosity	m ² /s	1×10 ⁻⁶
Gravitational acceleration	m/s ²	-9.81
Time step	s	1×10 ⁻⁴
Particle spacing	m	0.01
Particle number	-	35924

Table 2. DEM parameters in the simulation of submarine landslide

Parameter	Unit	Value
Spring constant	N/m	7×10 ⁸
Damping coefficient	N·s ² /m	3.5×10 ⁴
friction coefficient	-	0.27
Time step	s	1×10 ⁻⁶
Particle number	-	147

Fig. 3 presents the vertical displacement of the rigid landslide. The numerical results are in good agreement experimental data, which indicates that developed method can simulate the solid-solid interaction accurately during the slide process.

Fig. 4 shows the free surface elevations at $t = 0.5$ s and $t = 1.0$ s. Although the wave elevations near the rigid slide by MPS-DEM is obviously lower than that by experiment when $t = 0.5$ s. It can be noticed that the free surface profiles obtained by MPS-DEM match well with the experimental data in general.

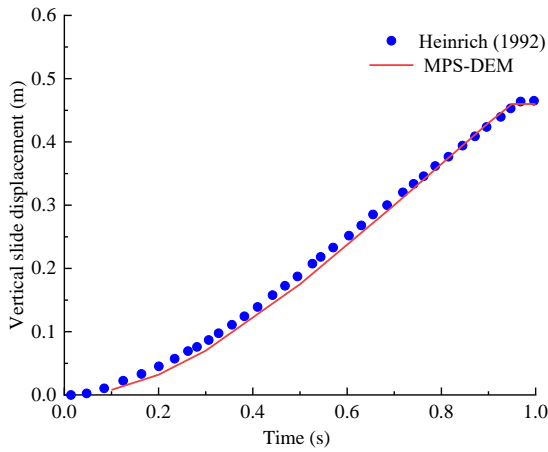
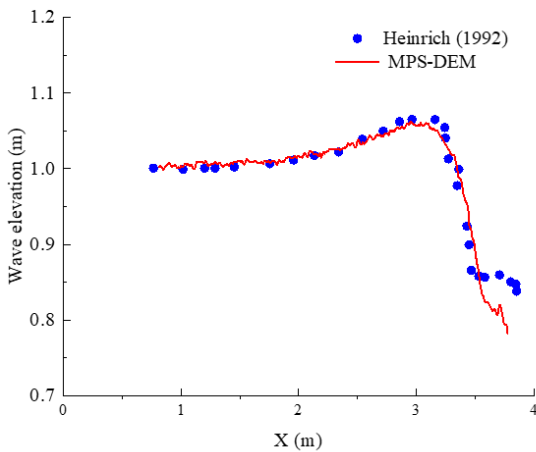
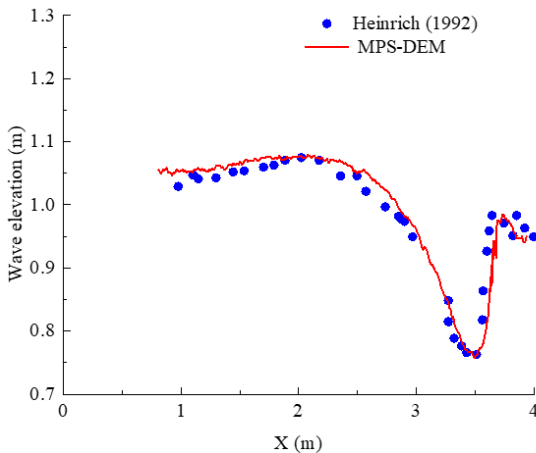


Fig. 3 Vertical displacement time histories of the rigid landslide measured by Heinrich (1992) and simulated by MPS-DEM - submarine rigid landslide



(a) $t = 0.5s$



(b) $t = 1.0s$

Fig. 4 Free surface elevations at (a) $t = 0.5s$ and (b) $t = 1.0s$ measured by Heinrich (1992) and simulated by MPS-DEM - submarine rigid landslide

Fig. 5 presents snapshots of pressure field and wave evolution at different instants. It can be noted that the pressure field is very smooth. The pressure field far away from the ramp is rarely affected by the sliding process in the whole simulation, which is consistent with actual situation. When $t = 1.0$ s, an unphysical phenomenon can be observed. The fluid becomes detached from the vertical wall of the rigid slide. The negative pressure may exist, which is not considered in present work. The TIC technique (Lyu et al., 2021) will be implemented to MPS-DEM model to avoid this phenomenon.

Subaerial rigid landslide

In this sub-section, the subaerial landslide (Heinrich, 1992) is simulated. the sketch of the numerical model is presented in Fig. 6. The water depth is 0.4 m and the rigid slide is placed above the water surface initially. The friction coefficient is set to 0.36, which is slightly higher than that in the case of submarine rigid landslide. This is because the submarine rigid slide contact with the wet surface during the whole process, while the subaerial rigid landslide is in contact with the dry surface for a period of time. Other parameters are consistent with that in the simulation of submarine rigid landslide.

The numerical results agree with the experimental data in terms of vertical slide displacement as shown in Fig. 7. Fig. 8 shows the free surface elevations at different instants. Computational results basically coincide with the experimental data. The first wave simulated by MPS-DEM are in good agreement with experimental results in terms of phase and peaks. There are also some small discrepancies, which can be observed. The second wave in simulation propagates slower than that in experiment, while their peaks are coincident.

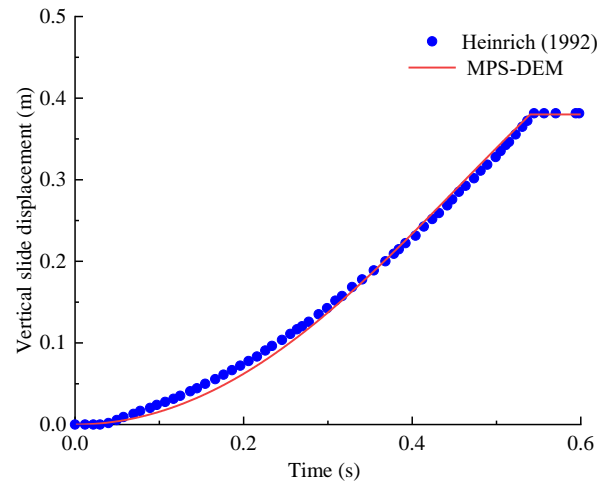


Fig. 7 Vertical displacement time histories of the rigid landslide measured by Heinrich (1992) and simulated by MPS-DEM - subaerial rigid landslide

Fig. 9 shows the snapshots of pressure field and wave evolution at different instants. Due to the sudden stop of slide, there is velocity difference between the rigid slide and fluid. Therefore, the fluid detaches from the slide at $t = 0.6s$. The first wave is generated at $t = 1.0s$ and the second wave is generated at $t = 1.5s$. The pressure field is changed dramatically with the travel of waves.

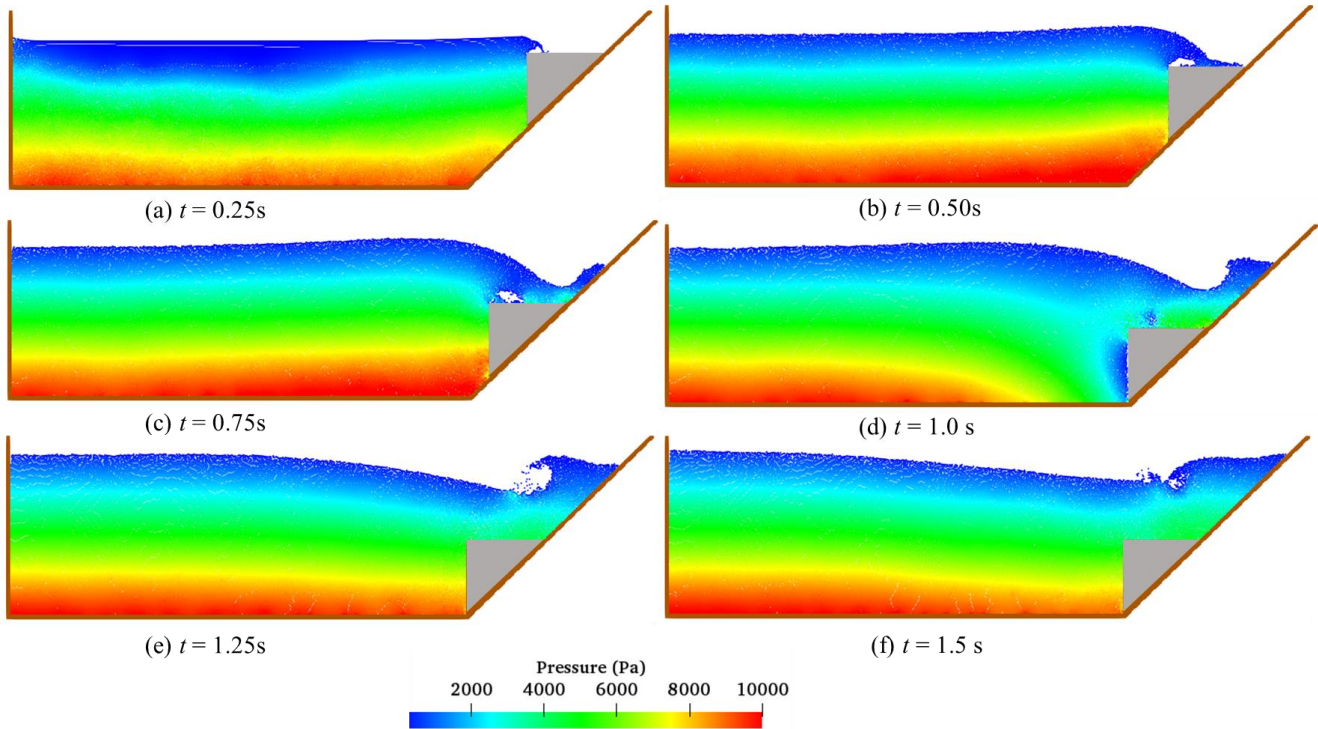


Fig. 5 Snapshots of pressure field and wave evolution at: (a) $t = 0.25s$, (b) $t = 0.5s$, (c) $t = 0.75s$, (d) $t = 1.0s$, (e) $t = 1.25s$, (f) $t = 1.5s$ - submarine rigid landslide

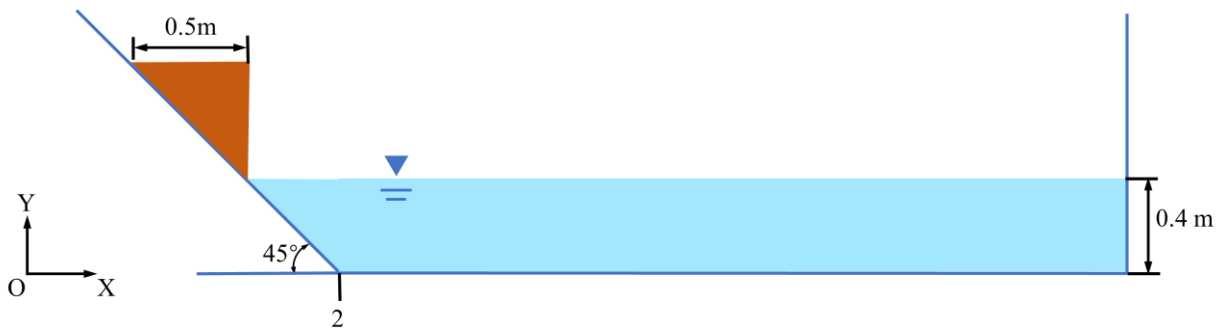


Fig. 6 Sketch of the numerical model for subaerial rigid landslide

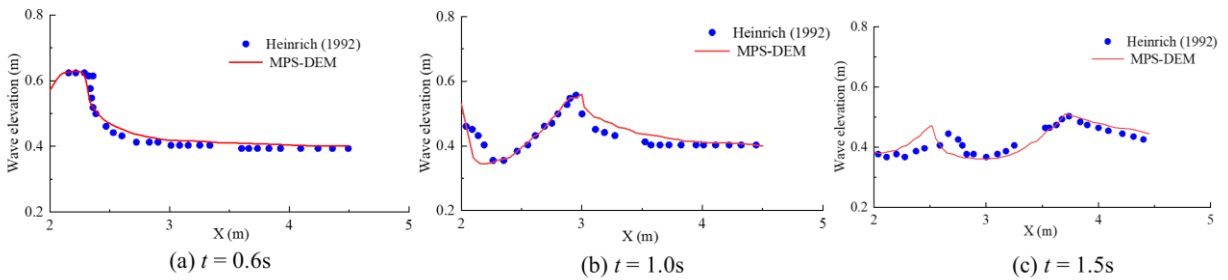


Fig. 8 Free surface elevations at (a) $t = 0.6s$, (b) $t = 1.0s$ and (c) $t = 1.5s$ measured by Heinrich (1992) and simulated by MPS-DEM – subaerial rigid landslide

CONCLUSIONS

In this paper, a fully Lagrangian meshless method MPS-DEM is developed to solve the fluid–solid interaction problem. The MPS method is employed to simulate the incompressible fluid flow, while

the DEM is used to build the solid-ramp interaction. Two simulations, including the submarine rigid landslide and subaerial rigid landslide, are conducted by MPS-DEM coupled method. The numerical result is in good agreement with experimental data, showing the accuracy of the coupled method. In the future, the model will be extended to a 3-D model and multi-bodies slide will be also considered.

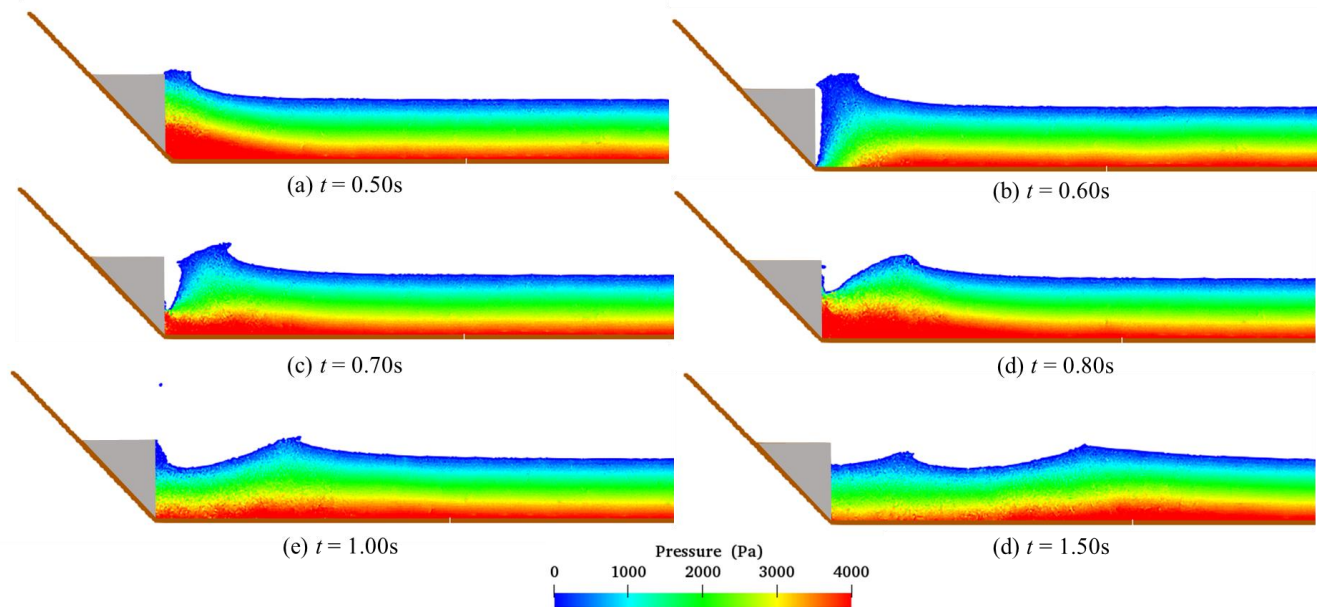


Fig. 9 Snapshots of pressure field and wave evolution at: (a) $t=0.50s$, (b) $t=0.60s$, (c) $t=0.70s$, (d) $t=0.80s$, (e) $t=1.00s$, (f) $t=1.50s$ - submarine rigid landslide

ACKNOWLEDGEMENTS

This work was supported by the National Natural Science Foundation of China (51879159, 52131102), and the National Key Research and Development Program of China (2019YFB1704200), to which the authors are most grateful.

REFERENCES

- Duan, G, Koshizuka, S, Yamaji, A, Chen, B, Li, X and Tamai, T (2018). "An accurate and stable multiphase moving particle semi-implicit method based on a corrective matrix for all particle interaction models." *Int J Numer Meth Eng*, 115(10): 1287-1314.
- Duan, G, Matsunaga, T, Yamaji, A, Koshizuka, S and Sakai, M (2021). "Imposing accurate wall boundary conditions in corrective-matrix-based moving particle semi-implicit method for free surface flow", *Int J Numer Meth Fluids*, 93:148-175.
- Gingold, RA, Monaghan, JJ (1977). "Smoothed particle hydrodynamics - theory and application to non-spherical stars," *Mon Not R Astron Soc*, 181(2), 375-389.
- Gotoh, H, Khayyer, A and Shimizu, Y (2021). "Entirely Lagrangian meshfree computational methods for hydroelastic fluid-structure interactions in ocean engineering—Reliability, adaptivity and generality," *Appl Ocean Res*, 115: 102822.
- Heinrich, P (1992). "Nonlinear Water Waves Generated by Submarine and Aerial Landslides," *J Waterway Port Coastal Ocean Eng*, 118(3): 249-266.
- Heller, V, Bruggemann, M, Spinneken, J, and Rogers, B-D (2016). "Composite modelling of subaerial landslide-tsunamis in different water body geometries and novel insight into slide and wave kinematics," *Coast Eng*, 109:20-41.
- Khayyer, A, Gotoh, H, (2011). "Enhancement of stability and accuracy of the moving particle semi-implicit method," *J Comput Phys*, 230(8): 3093-3118.
- Khayyer, A, Gotoh, H and Shimizu, Y (2017). Comparative study on accuracy and conservation properties of two particle regularization schemes and proposal of an optimized particle shifting scheme in ISPH context. *J Comput Phys*, 332: 236-256.
- Khayyer, A, Gotoh, H and Shimizu, Y (2019). "A projection-based particle method with optimized particle shifting for multiphase flows with large density ratios and discontinuous density fields," *Comput Fluids*, 179: 356-371.
- Khayyer, A, Gotoh, H, Shimizu, Y and Nishijima, Y (2021). "A 3D Lagrangian meshfree projection-based solver for hydroelastic Fluid-Structure Interactions," *J Fluid Struct*, 105: 103342.
- Khayyer, A, Gotoh, H, Shimizu, Y, Gotoh, K, Falahaty, H and Shao, S (2018). "Development of a projection-based SPH method for numerical wave flume with porous media of variable porosity," *Coast Eng*, 140:1-12.
- Koshizuka, S, Oka, Y (1996). "Moving-particle semi-implicit method for fragmentation of incompressible fluid," *Nucl Sci Eng*, 123, 421-434.
- Lin, P, Liu, X and Zhang, J (2015). "The simulation of a landslide-induced surge wave and its overtopping of a dam using a coupled ISPH model," *Eng Appl of Comp Fluid*, 9(1): 432-444.
- Liu, X, Morita, K and Zhang, S (2019). "A stable moving particle semi-implicit method with renormalized Laplacian model improved for incompressible free-surface flows," *Comput Methods Appl Mech Eng*, 356, 199-219.
- Lyu, HG, Sun, PN, Huang, XT, Chen, SH and Zhang, AM (2021). "On removing the numerical instability induced by negative pressures in SPH simulations of typical fluid-structure interaction problems in ocean engineering," *Appl Ocean Res*, 117: 102938.
- Qi, Y, Xu, Q, Chen, J, Zhang, J and Li, J (2022). "Study on solid block landslide generated tsunami using a modified δ -LES-SPH model," *Ocean Eng*, 245: 110473.
- Sun, PN, Colagrossi, A, Marrone, S, Antuono, M and Zhang, M (2019a). "A consistent approach to particle shifting in the δ -Plus-SPH model," *Comput Methods Appl Mech Eng* 348: 912-934.
- Sun, PN, Le Touze, D and Zhang, AM (2019b). "Study of a complex fluid-structure dam-breaking benchmark problem using a multi-phase SPH method with APR," *Eng Anal with Bound Elem*, 104: 240-258.
- Tanaka, M, Masunaga, T (2010). Stabilization and smoothing of pressure in MPS method by quasi-compressibility, *J Comput Phys*, 229(11): 4279-4290.

- Tan, H, Chen, S (2017). "A hybrid DEM-SPH model for deformable landslide and its generated surge waves," *Adv Water Resour*, 108: 256-276.
- Tan, H, Xu, Q and Chen, S 2018. "Subaerial rigid landslide-tsunamis: Insights from a block DEM-SPH model," *Eng Anal Bound Elem*, 95: 297-314.
- Wen, H, Ren, B and Wang, G, (2018). "3D SPH porous flow model for wave interaction with permeable structures," *Appl Ocean Res*, 75: 223-233.
- Wen, X., Zhao, W and Wan, DC (2021). "A multiphase MPS method for bubbly flows with complex interfaces," *Ocean Eng*, 238, 109743;
- Xu, WJ, Dong, XY (2021). "Simulation and verification of landslide tsunamis using a 3D SPH-DEM coupling method," *Comput Geotech*, 129: 103803.
- Xie, F, Zhao, W and Wan, DC (2020). "CFD simulations of three-dimensional violent sloshing flows in tanks based on MPS and GPU," *J Hydrodyn*, 32(4): 672-683.
- Xie, F, Zhao, W and Wan, DC (2021a). "MPS-DEM coupling method for interaction between fluid and thin elastic structures," *Ocean Eng*, 236, 109449.
- Xie, F, Zhao, W and Wan, DC (2021b). "Numerical simulations of liquid-solid flows with free surface by coupling IMPS and DEM," *Appl Ocean Res*. 104, 102771.
- Xu, R, Stansby, PK and Laurence, D (2009). "Accuracy and stability in incompressible SPH (ISPH) based on the projection method and a new approach," *J Comput Phys*, 228: 6703-6725.
- Yeylaghi, S, Moa, B, Buckham, B, Oshkai, P, Vasquez, J and Crawford, C 2017. "ISPH modelling of landslide generated waves for rigid and deformable slides in Newtonian and non-Newtonian reservoir fluids," *Adv Water Resour*, 107: 212-232.
- Zhang, G, Chen, J, Qi, Y, Li, J and Xu, Q (2021a). "Numerical simulation of landslide generated impulse waves using a δ^+ -LES-SPH model," *Adv Water Resour*, 151: 103890.
- Zhang, G, Zhao, W and Wan, DC (2021b). "Partitioned MPS-FEM method for free-surface flows interacting with deformable structures," *Appl Ocean Res*, 114, 102775.
- Zhang, Y, Wan, DC (2014). "Comparative study of MPS method and level-set method for sloshing flows," *J Hydrodyn*, 26(4): 577-585.
- Zhang, Y, Wan, DC (2017). "Numerical study of interactions between waves and free rolling body by IMPS method," *Comput Fluids*, 155: 124-133.
- Zhou, Q, Xu, WJ and Liu, GY (2021). "A contact detection algorithm for triangle boundary in GPU-based DEM and its application in a large-scale landslide," *Comput Geotech*, 138: 104371.